London South Bank University

MPhil Dissertation in

Petroleum Engineering

Department of Applied Science

Faculty of Engineering, Science and

The Built Environment (FESBE)

Research on Well Test Interpretation Model for Unconventional Tight Oil and Gas Reservoirs

Author: Zhao Zhang

Academic Supervisor: Professor Shiyi Zheng

Mode of Study: Full Time

Dissertation Submitted for the Degree of Master of Philosophy (MPhil) at London South Bank University

Date of Submission: 14-07-2015

ACKNOWLEGMENT

This dissertation is the end of my journey in obtaining my Master of Philosophy Degree in Petroleum Engineering. But in this journey I have not travelled alone. This study has been kept on track and seen through to completion with the support and encouragement of numerous people including my teachers, family and friends. At the end of my study, I would like to thank all those people who made this study possible and an unforgettable experience for me at London South Bank University.

First of all, I would like to express my sincere gratitude to my supervisor Professor Shiyi Zheng for the continuous support in study and research, for his patience, motivation, enthusiasm, and immense knowledge. His guidance helped me in the research and writing of this dissertation, I could not have imagined having a better advisor and mentor for my research than him.

Finally, I also would like to thank my parents for their spiritual support and encouragement.

Research on Well Test Interpretation Model for Unconventional Tight Oil and Gas Reservoirs

Zhao Zhang

Abstract

Unconventional energy resources have been characterized as those with large scale geometry and reserve, poor reservoir quality, which are difficult to evaluate and to apply the traditional techniques to develop for economic production. Unconventional oil and gas migration and flow mechanism dominate its exploration and development mode, which potentials are largely formation controlled. Very often, formation stimulation in unlocking the reservoir potential, such as fracturing technique is the key to develop unconventional reservoirs, such as the shale oil and gas, as well as the tight gas reservoirs. The state-of-art technology for tight oil and gas development is through long horizontal well with multi-stage fracturing.

Presented in this study, based on the thorough study of unconventional reservoirs matrix and fracture seepage mechanism, and considering the finite conductivity and infinite conductivity fractures; as well as the parameters such as fracturing completely penetrating or partially penetrating; perforation in the fractures and between fractures, fracture half length, fracture dipping, fracture spacing etc., the multi-stage fracturing horizontal well test interpretation models are established. The model takes into account broader factors and wide field application conditions, therefore, more robust than other published fractured horizontal well test models.

The current model for well test interpretation was solved using modern mathematical analysis methods. The type curves of multistage fracturing horizontal wells were generated. These type curves reflect the reservoir dynamic responses including those due to the main flow stage; the seepage flow characteristics of each stage, as well as the number of fractures, fracture half length, fracture conductivity, fracture inclination angle and other response characteristics. These type curves were then used by type curve matching methods to the well testing data from a field case, to calculate the reservoir and fracture parameters.

The field application and case study have shown that the developed well testing model can meet the actual production evaluation requirements, and the results are in good agreement with those published for unconventional tight oil and gas reservoir evaluation.

Keywords: unconventional, multi-stage fracturing, horizontal well, interpretation model, well test interpretation

Tables of Contents

List of Figures

Chapter 1

Introduction

Research on well test interpretation

Model for unconventional tight oil and gas reservoirs

Unconventional oil and gas resources include heavy oil, tight sandstone gas, coal-bed methane, shale gas and natural gas hydrate. Due to the huge amount of unconventional oil and gas, and as techniques become more and more economic in accordance to high international oil prices, making the unconventional oil and gas resources full of great development value. However, it is much more difficult in the method and techniques for exploration and development on unconventional oil and gas than that in conventional oil and gas, therefore, strengthening the research for the development of technology for oil and gas exploration of unconventional oil and gas, is the inevitable choice for sustainable development on tight oil and gas in twenty-first Century.

The tight sandstone oil and gas reserves of unconventional oil and gas reserves are huge, and the exploration and development techniques are the most mature in unconventional reservoirs, especially in the US, Canada, and China. All have made great economic benefits, and currently accounting for the first place of all global production in unconventional oil and gas.

Unconventional reservoir characteristics and hydrocarbon accumulation mechanism are different from the conventional oil and gas reservoirs, such as the large scale, poor reservoir properties, generally less than 10% porosity, and permeability less than $1 \times 10^{-3} \mu m^2$, therefore, the traditional production techniques usually cannot obtain the economic production.

Unconventional oil and gas migration and seepage mechanism determine its exploration and development mode, and fracturing technology is the key to shale oil and gas, tight oil (gas) and other unconventional oil and gas development. The long horizontal well multi-stage fracturing is the main development technique for

unconventional oil and gas reservoirs.

Multistage fracturing horizontal wells technology can effectively improve the near-wellbore flow conditions compared with vertical wells, so as to improve the well production; and it can effectively solve the problems such as multiple layers and thin beds; moreover, the multi-stage fracturing is equivalent to multiple straight well, and capable of greatly improving the controllable reserves. Currently, the multistage horizontal well fracturing technology on tight sandstone reservoirs has been successful, but the research on the multi stage fracturing of horizontal well testing model is still left behind. How many real effective fractures, after the completion of production are? How long is the actual effective fracture half-length? How about the actual conductivity of each fracture? How about the **pollution situation** around each fracture in the reservoir? and more other problems are all concerned by the developers. The well test analysis and interpretation can provide answers to these questions, in addition to the reservoir performance parameters.

This dissertation presents the study results of the well test interpretation model of tight sandstone reservoirs in unconventional reservoirs, giving full consideration on the actual situation of tight sandstone reservoir geological characteristics and fluid properties and other relevant characteristics. Through the test model of staged fracturing for horizontal wells, all kinds of external boundary conditions were considered, and the test analysis were conducted using field well testing data, so as to obtain the accurate formation parameters, and then provide a reasonable basis and solid foundation for the tight oil and gas field exploration and development.

Chapter 2

Study of multi-stage fracturing horizontal well

Physical model and flow regimes

2.1 The fracture formation mechanism

Horizontal well hydraulic fracturing has certain relationship between the reservoir and formation rock around the reservoir, mainly due to the properties of the rock mechanics. At first, the formation mechanism of fractures/fractures should be investigated.

Horizontal wellbore is controlled by three in-situ formation stress components, that is, the overburden pressure σ_v , maximum horizontal stress σ_H, minimum horizontal stress σ_h.

For the horizontal well fracturing system, artificial fracturing is generally divided into 3 kinds, transverse fracture, longitudinal fracture, horizontal fracture, as shown in Figure 1.

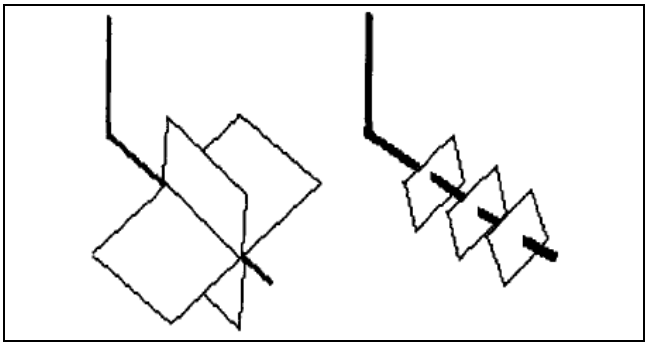

Longitudinal fracture Transverse fracture

Fig. 1 Schematic diagram of horizontal well fracture shape, where two type of likely combinations occurs in practice – cross-intersected fractures with horizontal well path (on the left), and parallel-intersected fractures with horizontal well path (on the right).

Transverse fractures are the fractures that are perpendicular to the horizontal well

bore, generally produce multiple transverse fractures; and longitudinal fractures are the fractures that are parallel to the horizontal well bore. For a horizontal well, what kind of actual fracturing will be produced is dependent on the formation stress.

Generally speaking, the minimum in-situ stress is in the horizontal direction, so the situation encountered in most is the transverse joint and longitudinal joint. If the wellbore is parallel to the minimum horizontal stress direction (i.e., along the direction of the minimum horizontal permeability), the transverse joints occur; if the horizontal wellbore crack perpendicular to the longitudinal direction of the minimum horizontal stress (i.e., along the direction of maximum horizontal permeability), then longitudinal fractures occur. Theoretical research and practical application show that the transvers fractures are better for production, than the longitudinal fractures. (Chen Wei et al., 2000).

Hydraulic fracturing is the process of generating artificially tensile failures along the wellbore wall/formation. The purpose is to expand the area of fluid flow region, and increase the oil production. The fracture initiation and fracture orientation depend on the order of the overburden pressure σ_v, maximum horizontal stress σ_H and minimum horizontal stress σ_h. As well as the horizontal well borehole axis position and rock mechanical properties. For the average reservoir depth, the general scale order of the stress component is $\sigma_H > \sigma_v > \sigma_h$ or $\sigma_v > \sigma_H > \sigma_h$.

Experimental studies and field tests yielded the following conclusions:

a. When the wellbore azimuth of horizontal wells and the principal stress direction are consistent, axial fracture will be produced; there may be horizontal fractures or vertical fractures, mainly depending on the size and the order of three stresses discussed above.

b. When the horizontal wellbore azimuth orientation oblique to the main ground stress, the space fracture is formed, and may give rise to complex fracture geometry.

c. Field test showed that the perforated section of the well that is four times less than the well borehole fracturing can generate transverse fractures; when the perforated interval is four times greater than borehole diameter, the fractures will be

multi-axial fracture group. In this study, the reason is given below for this phenomenon (Li Yongming et al., 2012).

The rock mechanics and reservoir engineering are combined to optimize the horizontal well fracturing program. For anisotropic permeability formations and low-permeability formations, the horizontal well fracturing is a good stimulation measure to increase production. Theoretical research and practical application show that the lateral fracture production is higher than the longitudinal fracture. Therefore, this dissertation mainly studies the well testing model for transverse fractures of a horizontal well.

2.2 The seepage mechanism of multistage fracturing horizontal wells

Horizontal well fracturing is the common means to change the fluid radial flow model of horizontal well to linear flow pattern. The characteristics of radial flow pattern are flow streamline converge to the well and highly concentrated along wellbore, and the bottom hole flow resistance is large. The characteristics of linear flow is a flow line parallel to the fractures in the formation walls, the flow resistance is much smaller.

Horizontal wells provide more drainage area for the implementation of low permeability reservoir stimulation technology. Through the implementation of multi-stage hydraulic fracturing horizontal wells, it is expected to further reduce the formation energy loss, and improve the productivity of the well.

For the uniform flow distribution assumption adopted in the fracture inflow, only accommodate the convenience of mathematical analysis, and inconsistent with the in-situ inflow of non-uniform distribution of fractures. Therefore, for the multiple fractures system in horizontal well, the fracturing should be studied and considered by taking into account of two most common situations, the infinite conductivity fractures and finite conductivity fractures. When small-scale fracturing produce short fracture or artificial fracture, the conductivity is high and the infinite conductivity fracture model can be approximately used (FAN Dong-yan et al., 2009).

The mechanism of fracturing seepage flow to increase production is explained by: changing from the radial flow of the formation fluid to the linear seepage. Radial flow

model is characterized by a streamline to well height concentration, and the bottom hole flow resistance is large, however, the characteristics of linear flow is a flow line parallel to the fractures in the formation walls, therefore, the flow resistance is relatively much smaller. After fracturing horizontal wells, their fluid flow process is divided into the following five stages:

2.2.1 The fracture linear flow

When the well is opened for a short time, the fluid flow direction is along the fracture towards the wellbore, the wellbore fluid is completely from the fractures, the layer outside of the fractures does not contribute to the fluid flow, the flow named the fracture linear flow, and this flow process is shown in Figure 2.

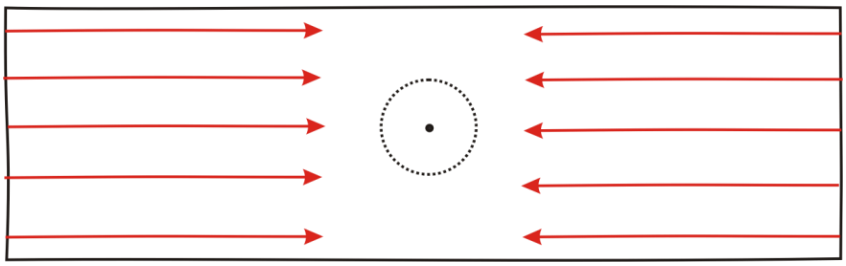

Fig. 2 Fracture linear flow – the cross-sectional view showing stream line of flow from formation matrix towards the horizontal well path.

2.2.2 The fracture formation of bilinear flow

Since the fluid within fractures storage is limited, and the fluid within the matrix perpendicular to the fracture gradually flows into the fractures, the fluid flows into the wellbore include that from fractures and that from the matrix flowing perpendicular to the fracture formation. Because the two linear flows exist at the same time, the flow is called the bilinear flow within fracture and formation, as shown in Figure 3.

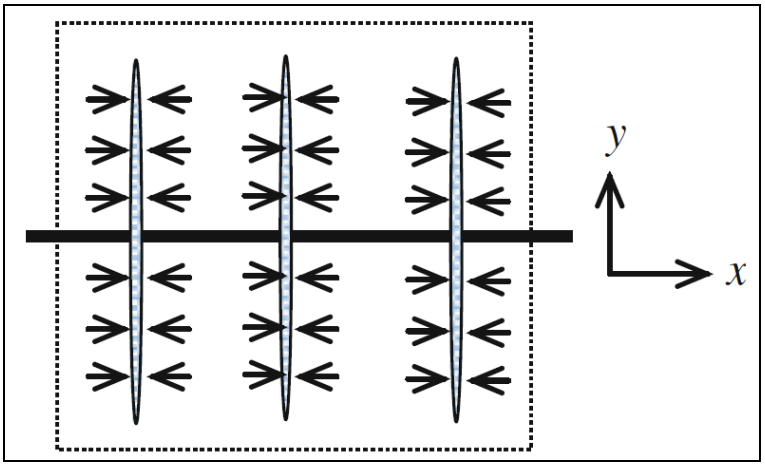

Fig. 3 fracture formation of bilinear flow, where linear flows in the fractures as well as from the formation matrix happened at the same time.

2.2.3 The fracture pseudo radial flow

With the expansion of the fluid flow ends within the fracture rock matrix system, the range of each fracture pressure is approximately circular, various fractures together intend to give rise to radial flow at later time, which is named pseudo-radial flow. However the interference between the fractures in the system is yet to come, depending on the flow at the fracture length and fracture spatial distribution. The fracture pseudo radial flow pattern is shown in Figure 4 below:

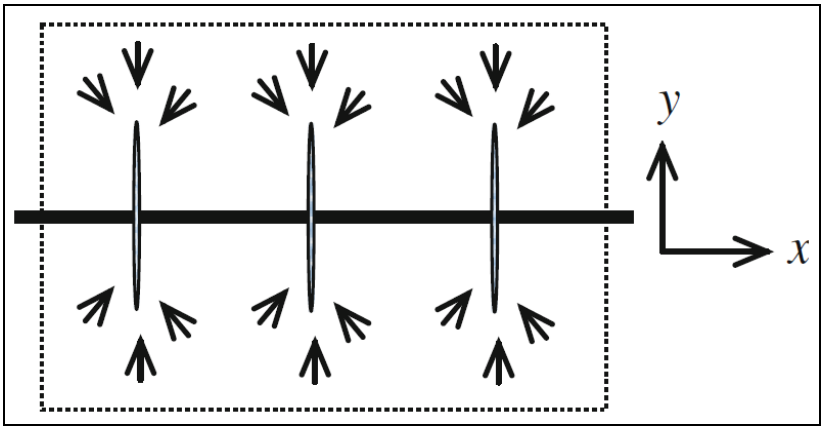

Fig. 4, Fracture pseudo radial flow, where flows from matrix towards horizontal well as well as converged to the tips of the fractures are shown.

2.2.4 The formation linear flow

After the production for a period of time, the matrix fractures for liquid can maintain stability, namely the fracture effect will gradually weaken after fracture linear flow and fracture of pseudo radial flow, the wellbore fluid seeps completely from the formation, then the formation fluid will flow in a linear fashion with major flows into the fractures, and forming the formation strata linear flow. This flow pattern is shown in Figure 5.

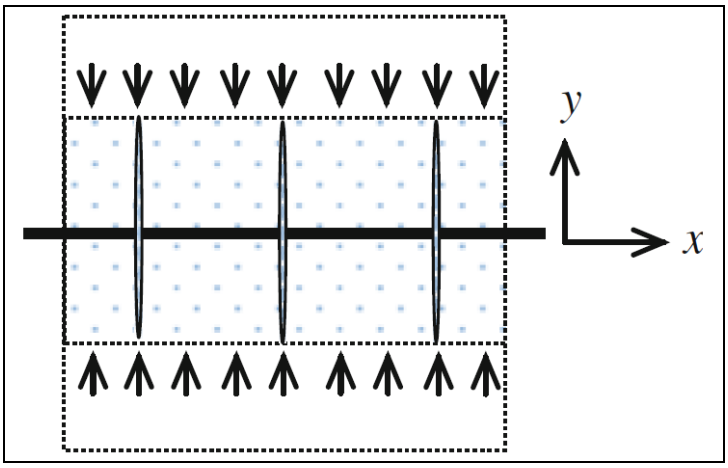

Figure 5, Formation linear flows, where in the region beyond the tips of the fractured zones, linear flows towards the region are shown with arrows.

2.2.5 The formation pseudo radial flow

With the further extension of the production time, the pressure wave is gradually extending outwards, a radial flow pattern, which is a little farther away from the horizontal well bore, is called formation pseudo radial flow. If the reservoir boundaries outside is infinite, pseudo-radial flow will form, as shown in Figure 6 (Sheng Ruyan et al.., 2003).

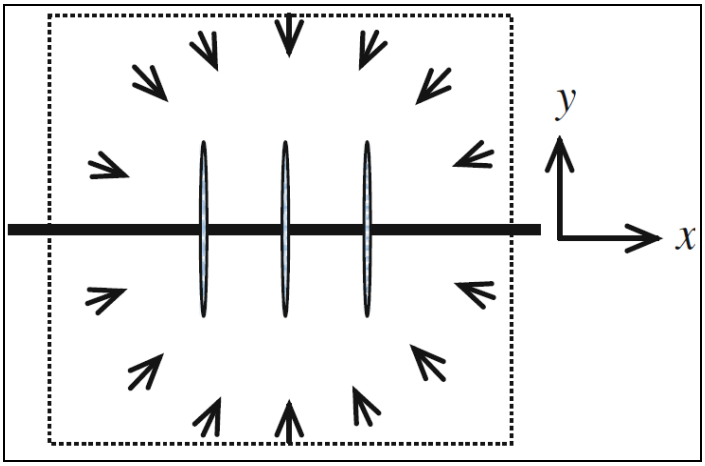

Figure 6 Formation pseudo radial flow, where far beyond the fractured regions, in a infinite acting reservoir, pseudo-radial flow towards the horizontal well as well as the fractured regions are shown.

Chapter 3

Research on well testing model for horizontal well with multiple fractures

For the thin interbedded reservoir of low permeability, it usually cannot reach the expected development performance by using only horizontal wells. Therefore, we often use the method of multiple hydraulic fracturing to increase the productivity of horizontal wells. The domestic scholars have grasped the flow characteristic of the fractured horizontal well with the application of the fractured horizontal well technology in the reservoirs.

On the basis of deep study on unconventional reservoir matrix and fracture flow mechanism, and considering the factors such as finite conductivity and infinite conductivity fractures percolation mode, fractures completely penetrating or partial penetrating, perforation in the fractures and between the fractures, fracture half length, tilting angle of the crack, crack spacing, etc. infinite acting, reservoir with closed rectangular boundary, constant pressure boundary, the bottom water support reservoir of multistage fracturing horizontal well test interpretation models are established.

This dissertation mainly introduces the finite conductivity and infinite conductivity fractures in infinite acting reservoir of multistage fracturing horizontal well test interpretation models (Zerzar et al., 2003).

3.1 Well testing model for horizontal well with multiple fractures of Infinite conductivity

3.1.1 Physical model

The schematic diagram of the model for the multi-stage fracturing horizontal well is shown in Figure 7, assuming that:

(1) The reservoir thickness is h, the wellbore position to the upper and lower boundaries is Zw, and the horizontal well length is L.

(2) The reservoir is homogeneous, anisotropic and infinite size. The thickness is uniform. The top surface and the bottom surface are closed, no-flow boundaries.

(3) The horizontal well is penetrated by m longitudinal fractures that are non-deformable (Figures 8 and 9). The fracture half-length is y_f. The fracture height is h_f. The angle between the fracture plane and the horizontal plane of the wellbore is αj. The fluid flows into the wellbore from the fracture surface only (y-z plane). No fluid flows through the end of the fractures.

(4) The flow rate is constant in the bottom of the horizontal well, but the flow rate qj of each crack is not necessarily equal (the horizontal well produces at constant production rate of q).

(5) The formation rock and fluid are slightly compressible, and the compression coefficient is constant, the crude oil viscosity is constant.

(6) The fluid flow is infinite conductivity in the horizontal wellbore and the fractures. The fluid flows into the fractures once and instantaneously flows into the wellbore.

(7) The fluid flows under Darcy law in reservoir.

(8) Ignore the effect of gravity and capillary force, and considering the effect of wellbore storage and skin (Zheng, 1998).

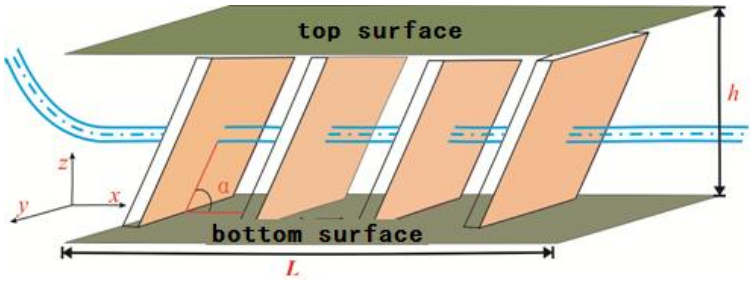

Figure7, Schematic diagram of flow model for multi-stage fracturing horizontal well, with no-flow boundaries at the top and bottom of the reservoir.

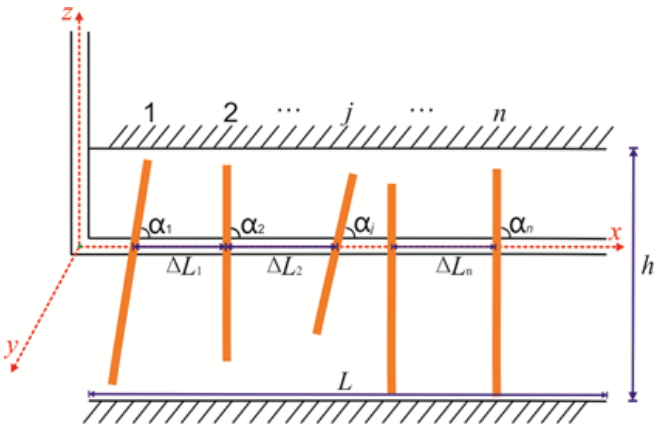

Figure 8, X-Z plane front views of ideal horizontal well path with a length of L, with intersected fractures at different angles.

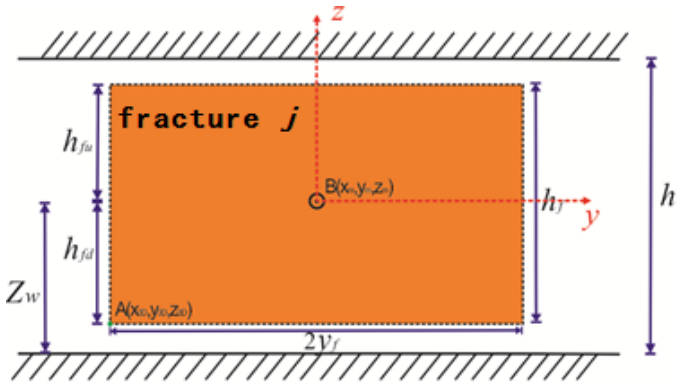

Figure 9, Y-Z plane side views showing the horizontal well (in a circle), intersected by the fracture plane (brown colour). Z_w denotes the horizontal well position between formation layers with a thickness of h.

3.1.2 Mathematical model

In the three-dimensional Cartesian coordinates, the control differential equation is given below (Brown et al., 2009):

$$\frac{K_x}{\mu}\frac{\partial^2 p}{\partial x^2}+\frac{K_y}{\mu}\frac{\partial^2 p}{\partial y^2}+\frac{K_z}{\mu}\frac{\partial^2 p}{\partial z^2}=\phi C_t\frac{\partial p}{\partial t} \qquad (x,y,z)\in\Omega, t>0$$

Initial condition:

$$p(x,y,z,0)=p_i$$

Outer boundary conditions:

$$\lim_{|x|\to\infty} p=p_i, \lim_{|x|\to\infty}\frac{\partial p}{\partial x}=0 \qquad t\geq 0$$

$$\lim_{|y|\to\infty} p=p_i, \lim_{|y|\to\infty}\frac{\partial p}{\partial y}=0 \qquad t\geq 0$$

Closed bottom surface:

$$\frac{\partial p(x,y,z,t)}{\partial z}|_{z=0}=0$$

Closed top surface:

$$\frac{\partial p(x,y,z,t)}{\partial z}|_{z=h}=0$$

Where:

$\tilde{q}$ —— point source output, m^3/d δ ( ) —— δ function

K_x，K_y，K_z—— x，y，z direction of permeability, μm^2 P —— for pressure, *Mpa*

p_i —— for initial formation pressure, *Mpa*, t —— time, *h*

μ —— viscosity, *mPa·s* $Ø$ —— porosity

C_t —— total compressibility, MPa^{-1} h —— formation thickness，*m*

3.1.3 Dimensionless mathematical model

For the convenience of type curve generation and analysis, math model and solutions in dimensionless form are often used. The dimensionless parameters are defined as followings (hang Ziming, 2009):

The dimensionless pressure is defined as：

$$p_{\mathrm{D}}=\frac{h\sqrt{K_x K_y}}{1.842\times10^{-3}q\mu B}(p_i-p)$$

The dimensionless time is defined as：

$$t_{\mathrm{D}}=\frac{3.6K_z t}{\phi\mu C_t h^2}$$

The dimensionless distance is defined as:

$$x_{\mathrm{D}}=\frac{x}{h}\sqrt{\frac{K_z}{K_x}},y_{\mathrm{D}}=\frac{y}{h}\sqrt{\frac{K_z}{K_y}},z_{\mathrm{D}}=\frac{z}{h},$$

$$x_{\mathrm{wD}}=\frac{x_{\mathrm{w}}}{h}\sqrt{\frac{K_z}{K_x}},y_{\mathrm{wD}}=\frac{y_{\mathrm{w}}}{h}\sqrt{\frac{K_z}{K_y}},z_{\mathrm{wD}}=\frac{z_{\mathrm{w}}}{h},$$

$$x_{\mathrm{AjD}}=\frac{x_{\mathrm{Aj}}}{h}\sqrt{\frac{K_z}{K_x}},y_{\mathrm{AjD}}=\frac{y_{\mathrm{Aj}}}{h}\sqrt{\frac{K_z}{K_y}},z_{\mathrm{AjD}}=\frac{z_{\mathrm{Aj}}}{h},$$

$$x_{\mathrm{BjD}}=\frac{x_{\mathrm{Bj}}}{h}\sqrt{\frac{K_z}{K_x}},y_{\mathrm{BjD}}=\frac{y_{\mathrm{Bj}}}{h}\sqrt{\frac{K_z}{K_y}},z_{\mathrm{BjD}}=\frac{z_{\mathrm{Bj}}}{h},$$

$$y_{\mathrm{fjD}}=\frac{y_{\mathrm{fj}}}{h}\sqrt{\frac{K_z}{K_y}},h_{\mathrm{fjD}}=\frac{h_{\mathrm{fj}}}{h},$$

$$\Delta L_{j\mathrm{D}}=\frac{\Delta L_j}{h}\sqrt{\frac{K_z}{K_x}},L_{\mathrm{D}}=\frac{L}{h}\sqrt{\frac{K_z}{K_x}}$$

The dimensionless wellbore storage coefficient is defined as:

$$C_{\mathrm{D}}=\frac{C}{\phi C_t h^3}\sqrt{\frac{K_z^2}{K_x K_y}}$$

where：

p_{D} —— dimensionless pressure t_{D} —— dimensionless time

$q_{j\mathrm{D}}$——dimensionless rate of the j fracture

x_{D}， y_{D}， z_{D} —— dimensionless distance of a point on (x, y, z) in the space in x, y, z direction

x_{wD}， y_{wD}， z_{wD} —— dimensionless distance of a point on (x_w， y_w， z_w) on the wellbore in x, y, z direction

$x_{\mathrm{A}j\mathrm{D}}$， $y_{\mathrm{A}j\mathrm{D}}$， $z_{\mathrm{A}j\mathrm{D}}$ ——dimensionless distance of A point on ($x_{\mathrm{A}j}$， $y_{\mathrm{A}j}$， z_{A}) in x, y, z direction

$x_{\mathrm{B}j\mathrm{D}}$， $y_{\mathrm{B}j\mathrm{D}}$， $z_{\mathrm{B}j\mathrm{D}}$ —— dimensionless distance of B point on ($x_{\mathrm{B}j}$， $y_{\mathrm{B}j}$， z_{B}) in x, y, z direction

$y_{\mathrm{f}j}$ ——fracture half length of the j fracture, *m*

$y_{\mathrm{f}j\mathrm{D}}$ —— dimensionless fracture half length of the j fracture

$h_{\mathrm{f}j}$ —— fracture half height of the j fracture, *m*

$h_{\mathrm{f}j\mathrm{D}}$ —— dimensionless fracture half height of the j fracture

ΔL_j —— distance between the j fracture and the (j+1) fracture, *m*

$\Delta L_{j\mathrm{D}}$ —— dimensionless distance between the j fracture and the (j+1) fracture

L ——length of the horizontal well, *m*

L_{D} —— dimensionless length of the horizontal well

C ——wellbore storage coefficient, m^3/MPa

C_{D} —— dimensionless wellbore storage coefficient

In the three-dimensional Cartesian coordinates, the dimensionless control differential equation of the point source of the multi-stage fracturing horizontal well flow is written as:

$$\frac{\partial^2 p_D}{\partial {x_D}^2}+\frac{\partial^2 p_D}{\partial {y_D}^2}+\frac{\partial^2 p_D}{\partial {z_D}^2}+\tilde{q}_D\delta(x_D-x_{wD},y_D-y_{wD},z_D-z_{wD})=\frac{\partial p_D}{\partial t_D}$$

Initial condition:

$$p_D(x_D,y_D,z_D,0)=0$$

Outer boundary conditions:

$$\lim_{|x_D|\to\infty} p_D=0,\ \lim_{|x_D|\to\infty}\frac{\partial p_D}{\partial x_D}=0$$

$$\lim_{|y_D|\to\infty} p_D=0,\ \lim_{|y_D|\to\infty}\frac{\partial p_D}{\partial y_D}=0$$

Closed bottom surface:

$$\frac{\partial p_D(x_D,y_D,z_D,t_D)}{\partial z_D}|_{z_D=0}=0$$

Closed top surface:

$$\frac{\partial p_D(x_D,y_D,z_D,t_D)}{\partial z_D}|_{z_D=1}=0$$

3.1.4 Mathematical model analytical solution

In the multistage fracturing horizontal well, according to the characteristics of

the dimensionless point source seepage of the differential equation, and the boundary conditions, the mathematical problem is to solve the partial differential equations. Using the orthogonal transformation, the problem can be converted to the initial value problems of ordinary differential equations, and then based on the basic theory of matrix differential equation; we can calculate the exact solution of the problem. Considering the three-dimensional characteristic values, the converted equations are shown as follows (Roumboutsos et al., 1988):

$$\begin{cases} \dfrac{\partial^2 E}{\partial {x_{\mathrm{D}}}^2}+\dfrac{\partial^2 E}{\partial {y_{\mathrm{D}}}^2}+\dfrac{\partial^2 E}{\partial {z_{\mathrm{D}}}^2}=-\lambda E,(x_{\mathrm{D}},y_{\mathrm{D}})\in R^2,0<z_{\mathrm{D}}<1 \\ p_{\mathrm{D}}(x_{\mathrm{D}},y_{\mathrm{D}},z_{\mathrm{D}},0)=0 \\ \dfrac{\partial E}{\partial z_{\mathrm{D}}}|_{z_{\mathrm{D}}=0}=\dfrac{\partial E}{\partial z_{\mathrm{D}}}|_{z_{\mathrm{D}}=1}=0 \\ \lim\limits_{|x_{\mathrm{D}}|\to\infty} E=0,\ \lim\limits_{|x_{\mathrm{D}}|\to\infty}\dfrac{\partial E}{\partial x_{\mathrm{D}}}=0 \\ \lim\limits_{|y_{\mathrm{D}}|\to\infty} E=0,\ \lim\limits_{|y_{\mathrm{D}}|\to\infty}\dfrac{\partial E}{\partial y_{\mathrm{D}}}=0 \end{cases}$$

Exact solution is introduced for the dimensionless orthogonal transformation, and the multi-stage fracturing horizontal wells bottomhole pressure, that is, the whole point of the space Ω source solution is:

$$p_{\mathrm{D}}(x_{\mathrm{D}},y_{\mathrm{D}},z_{\mathrm{D}},t_{\mathrm{D}})=\frac{q_{\mathrm{D}}}{2\pi}\int_0^{t_{\mathrm{D}}}\frac{1}{\tau}\mathrm{e}^{-\frac{1}{4\tau}(x_{\mathrm{wD}}-x_{\mathrm{D}})^2}\mathrm{e}^{-\frac{1}{4\tau}(y_{\mathrm{wD}}-y_{\mathrm{D}})^2} \sum_{n=0}^{\infty}\frac{1}{A_n}\cos(n\pi z_{\mathrm{wD}})\cos(n\pi z_{\mathrm{D}})\mathrm{e}^{-(n\pi)^2\tau}d\tau$$

Any influence of fracture j (as shown in Figure 10) on the target point (x_{D},y_{D},z_{D}) pressure influence, is obtained by the point source solution must be extended to the whole fracture plane, that's the type of point source solution for fracture plane (x,z plane) integral, the target pressure expression is:

$$p_{jD}(x_D, y_D, z_D, t_D)$$
$$= \frac{q_{jD}}{2\pi}\int_0^{t_D}\frac{1}{\tau}\int_0^1 e^{-\frac{(y_{AjD}+2\sigma y_{fjD}-y_D)^2}{4\tau}} d\sigma$$
$$\sum_{n=0}^{\infty}\frac{1}{A_n}\{\int_0^1 e^{-\frac{(x_{AjD}+2\xi h_{fjD}\cos\alpha_j - x_D)^2}{4\tau}}\cos[n\pi(z_{AjD}+\xi h_{fjD}\sin\alpha_j)]d\xi\}$$
$$\cos(n\pi z_D)e^{-(n\pi)^2\tau}d\tau$$

Where: the $p_{jD}(x_D, y_D, z_D)$ is only the first j fractures, pressure point (x_D, y_D, z_D). τ, σ, ξ is the integral variables.

According to the physical model assumption, horizontal well fracturing have m fractures, the target (x_D, y_D, z_D) should be affected by pressure of the m fractures, strict expression for its target is:

$$p_D(x_D, y_D, z_D, t_D)$$
$$= \sum_{j=1}^{m}\frac{q_{jD}}{2\pi}\int_0^{t_D}\frac{1}{\tau}\int_0^1 e^{-\frac{(y_{AjD}+2\sigma y_{fjD}-y_D)^2}{4\tau}} d\sigma$$
$$\sum_{n=0}^{\infty}\frac{1}{A_n}\{\int_0^1 e^{-\frac{(x_{AjD}+\xi h_{fjD}\cos\alpha_j - x_D)^2}{4\tau}}\cos[n\pi(z_{AjD}+\xi h_{fjD}\sin\alpha_j)]d\xi\}$$
$$\cos(n\pi z_D)e^{-(n\pi)^2\tau}d\tau$$

Where: $p_D(x_D, y_D, z_D)$ is the point (x_D,y_D,z_D) pressure when there are m fractures.

For each of the fractures that have different production q_j, the pressure from cross point of j[th] fractures with horizontal intersection at $B_j(x_{BjD}, y_{BjD}, z_{BjD})$ is:

$$p_{BjD}(x_{BjD}, y_{BjD}, z_{BjD}, t_D)$$
$$= \sum_{j=1}^{m}\frac{q_{jD}}{2\pi}\int_0^{t_D}\frac{1}{\tau}\int_0^1 e^{-\frac{(y_{AjD}+2\sigma y_{fjD}-y_{BjD})^2}{4\tau}} d\sigma$$
$$\sum_{n=0}^{\infty}\frac{1}{A_n}\{\int_0^1 e^{-\frac{(x_{AjD}+\xi h_{fjD}\cos\alpha_j - x_{BjD})^2}{4\tau}}\cos[n\pi(z_{AjD}+\xi h_{fjD}\sin\alpha_j)]d\xi\}$$
$$\cos(n\pi z_{BjD})e^{-(n\pi)^2\tau}d\tau$$

Where: p_{BjD} (x_D,y_D,z_D) is the B_j(x_{BjD}, y_{BjD}, z_{BjD}) pressure when there are m fractures.

Assuming that the wellbore and fracture are infinite seepage, the pressure of each point in the wellbore and fracture is equal everywhere, so:

$$
\begin{aligned}
p_{wD}(t_D) &= p_{BjD}(x_{BjD}, y_{BjD}, z_{BjD}, t_D) \\
&= \sum_{j=1}^{m} \frac{q_{jD}}{2\pi} \int_0^{t_D} \frac{1}{\tau} \int_0^1 e^{-\frac{(y_{AjD}+2\sigma y_{fjD}-y_{BjD})^2}{4\tau}} d\sigma \\
&\quad \sum_{n=0}^{\infty} \frac{1}{A_n} \{ \int_0^1 e^{-\frac{(x_{AjD}+\xi h_{fjD}\cos\alpha_j - x_{BjD})^2}{4\tau}} \cos[n\pi(z_{AjD} + \xi h_{fjD}\sin\alpha_j)] d\xi \} \\
&\quad \cos(n\pi z_{BjD}) e^{-(n\pi)^2 \tau} d\tau
\end{aligned}
$$

Where: the p_{wD} is bottom hole pressure of multi-segment fracturing horizontal well.

In the equations above, there are m+1unknown parameters: m q_{jD} and p_{wD}. To solve the m+1 question, we must add an equation, according to the assumption of horizontal wells for production output at q, so:

$$\sum_{j=1}^{m} q_{jD} = 1$$

Solving the equations above together with a total of m+1 equations and m+1 unknowns, we can get more exact solutions for pressure response from fracturing horizontal well.

Solutions obtained above have not considered the wellbore storage effect and skin effect, if we take account of the wellbore storage effect and skin factor (total skin factor), it is necessary to take the following steps: first, finding out the exact solution of bottom hole pressure, and then transformation to the Laplace space under the bottom hole pressure according to the principle of superposition of Duhamel:

$$\bar{p}_{\mathrm{wD}}(C_{\mathrm{D}},S,u)=\frac{\bar{p}_{\mathrm{wD}}(u)+\dfrac{S}{2\pi uL_{\mathrm{D}}}}{1+\dfrac{uC_{\mathrm{D}}S}{2\pi L_{\mathrm{D}}}+u^{2}C_{\mathrm{D}}\bar{p}_{\mathrm{wD}}(u)}$$

Where: $\bar{p}_{\mathrm{wD}}(u)$ is the exact solution of bottom-hole pressure as a function of transformation.

$\bar{p}_{\mathrm{wD}}(C_{\mathrm{D}},S,u)$ is the function of bottom-hole pressure in Laplace space.

Finally, using Stehfest numerical inversion method, the Laplace space under the bottom-hole pressure $\bar{p}_{\mathrm{wD}}(C_{\mathrm{D}},S,u)$ is transformed to real space to give dimensionless bottom hole pressure $p_{\mathrm{wD}}(C_{\mathrm{D}},S,t_{\mathrm{D}})$ of multi-stage fractured horizontal well.

3.1.5 Type curves

Figure 10 is the multi-segment fracturing horizontal well dimensionless bottom hole pressure and pressure derivatives double logarithm plot; Figure 11 shows the flow patterns/forms diagram of multi-stage fracturing horizontal well. (Stehfest, H, 1970)

It can be seen from the Figure 10 that, the double logarithm diagnostic plot is mainly divided into five segments (the fluid flow in formation is mainly divided into following several stages):

① The first stage, mainly due to the impact of wellbore storage, the overlap of the pressure and pressure derivative straight lines' slope is 1, and then the pressure derivative with a "hump" characteristics.

② The second stage, which is early fracture linear flow, the main features of the pressure derivative curve slope is 0.5, the fluid along the fractures surface with a linear flow regime, various fractures flow independently, and the fluid flow configuration diagram is shown in Figure 11 (a).

③ The third stage, which is the early fractures of radial flow period, the pressure derivative curve is the horizontal line, along with the extension

fracture tip flow, the pressure of formation fractures in various extents is approximately circular, and characterized by a radial fluid flow, however, the interference between fractures does not occur. If the fracture spacing is short, or fractures are high, the response with interference would be very different. The flow pattern without interference is shown in Figure 11 (b).

④ The fourth stage, which is the linear flow section in formation, the pressure derivative curve slope is 0.36, and flow interference occurs, the fluid flow is shown in Figure 11 (c).

⑤ The fifth stage, which is a composite/pseudo- radial flow stage, the pressure derivative is horizontal line at 0.5, the flow is shown in Figure 11 (d).

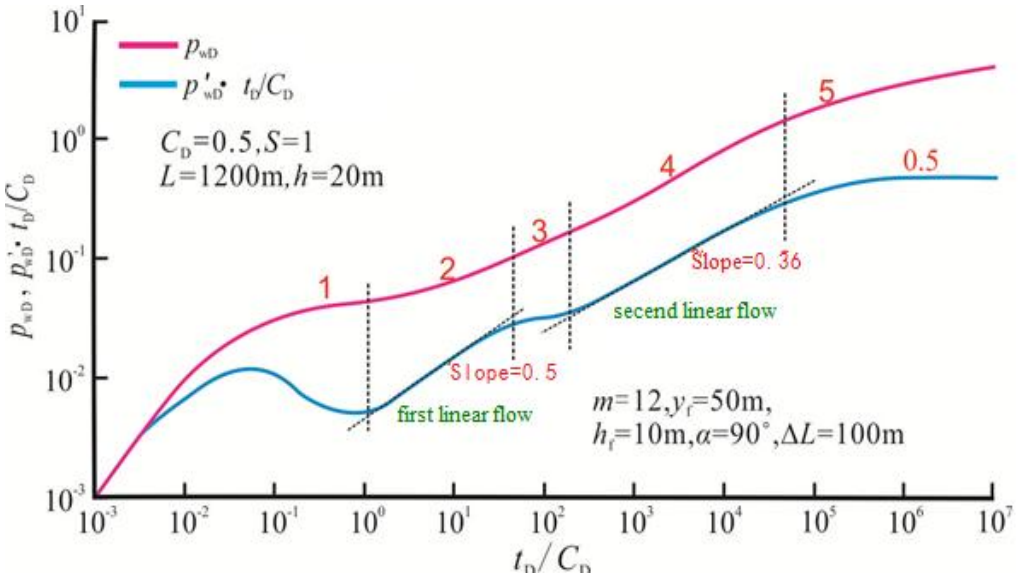

Figure 10 Type curves of multistage fracturing horizontal well. Horizontal axis is dimensionless time, t_D/C_D, while the vertical axis denotes the dimensionless pressure and logarithmic derivatives, i.e. P_{wD} and P'_{wD}.

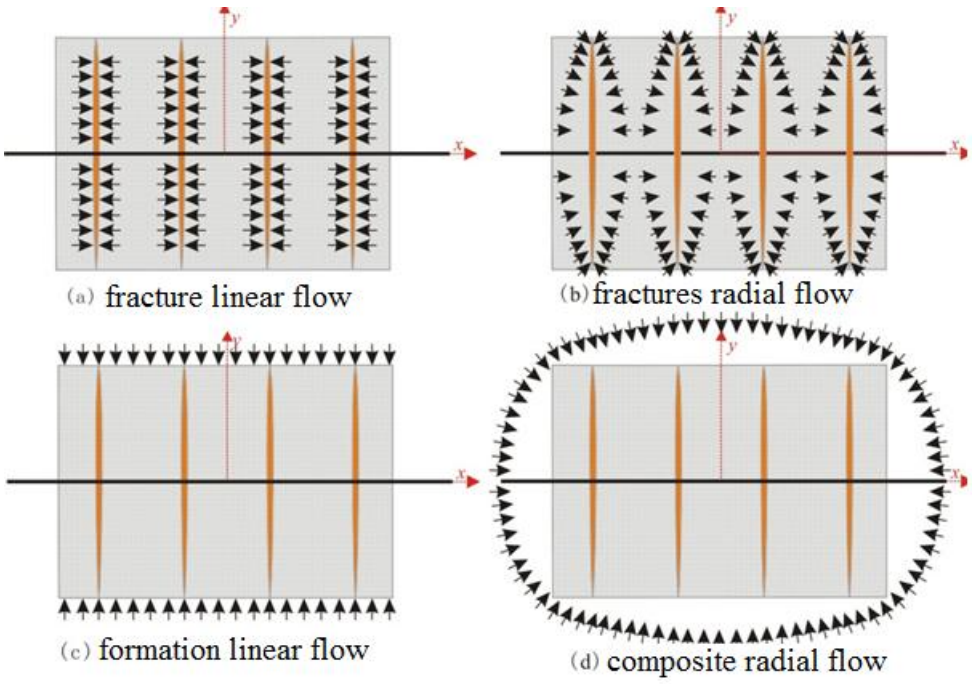

Figure 11, the flow patterns/forms diagram of multi-stage fracturing horizontal well, where fracture linear flow, radial flow as well as formation linear flow and composite/pseudo-radial flow are shown.

3.1.6 Sensitivity analysis

Figure 12 is the well test Type curves considering the effect of fracture numbers on multistage fracturing horizontal well. It can be seen that with the increase of the fracture numbers, the double logarithmic graph of pressure and pressure derivative curve shows downward trend, and the impact on the pressure derivative curve occurs mainly in the early fracture linear flow.

The Figure 13 shows that the longer the fracture half length, the longer the stage of fracture linear flow, the earlier the interference between the fractures occurs, and when the fracture half length increases to a certain length, the fracture formation pseudo radial flow cannot be formed.

It can be seen from the Figure 14 that, in early fracture linear flow and radial flow stage, with the increase of the fracture height, and fracturing pressure derivative curve tends to drop downward.

It can be seen in Figure 15 that, with the decrease of fracture dip angle, the pressure and pressure derivative curve drops as well, the pressure derivative curve in fracture linear flow and fracture radial flow periods are more sensitive.

Figure 16 is the effect of fracture spacing on multistage fracturing horizontal well test Type curves, the influence is mainly in the phase of fracture pseudo radial flow and formation fracture linear flow. When the fracture spacing is smaller than a certain value, the fracture radial flow stage cannot be reflected in the derivative curve.

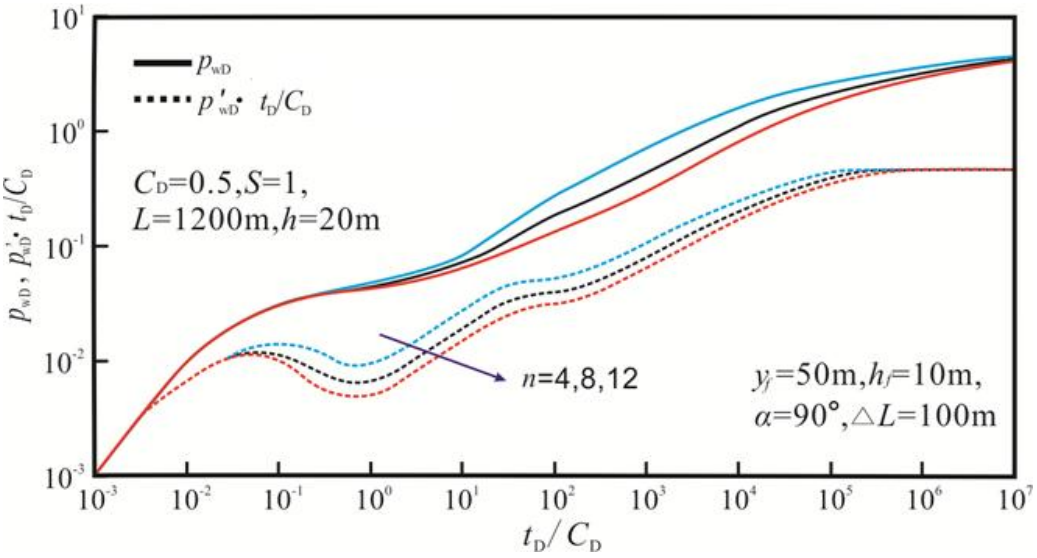

Figure 12, Effect of fracture numbers on multistage fracturing horizontal well test Type curves, where the arrow on the derivative curve shows the trend of changes of flow with the increase of the fracture numbers (n: 4, 8 and 12).

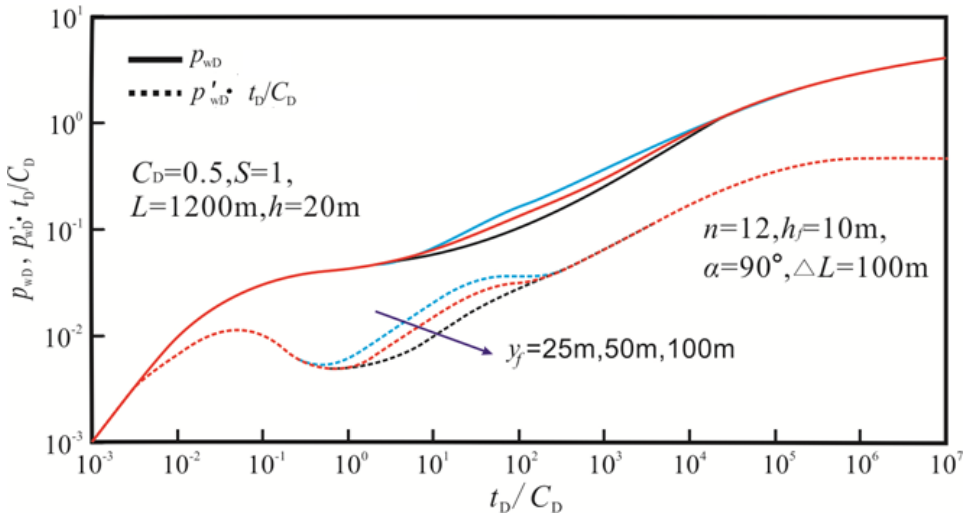

Figure 13, Effect of fracture half length on multistage fracturing horizontal well test Type curves, where half length (y_f) changed from 25m; 50m and 100m.

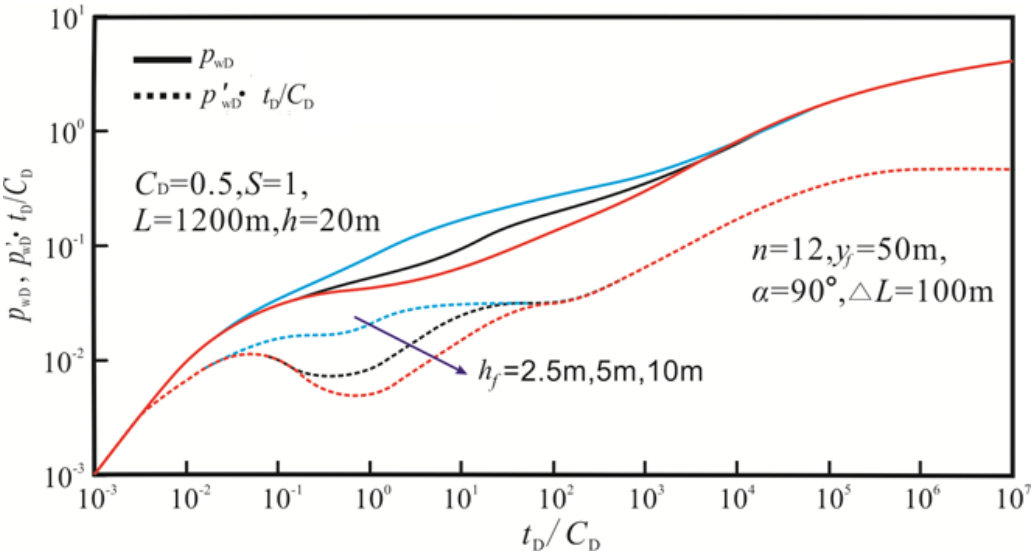

Figure 14, Effect of fracture height on multistage fracturing horizontal well test Type curves, where fracture height (h_f) changed from 2.5m; 5m and 10m respectively.

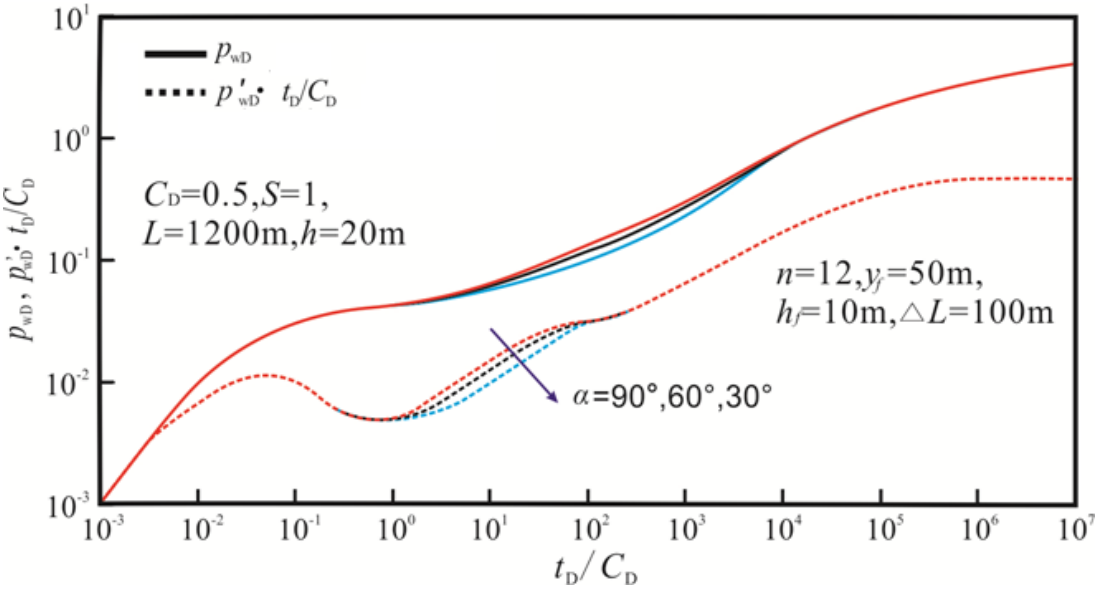

Figure 15, Effect of fracture dip on multistage fracturing horizontal well test Type Curves, which was changed from 90^0 – 30^0 degrees.

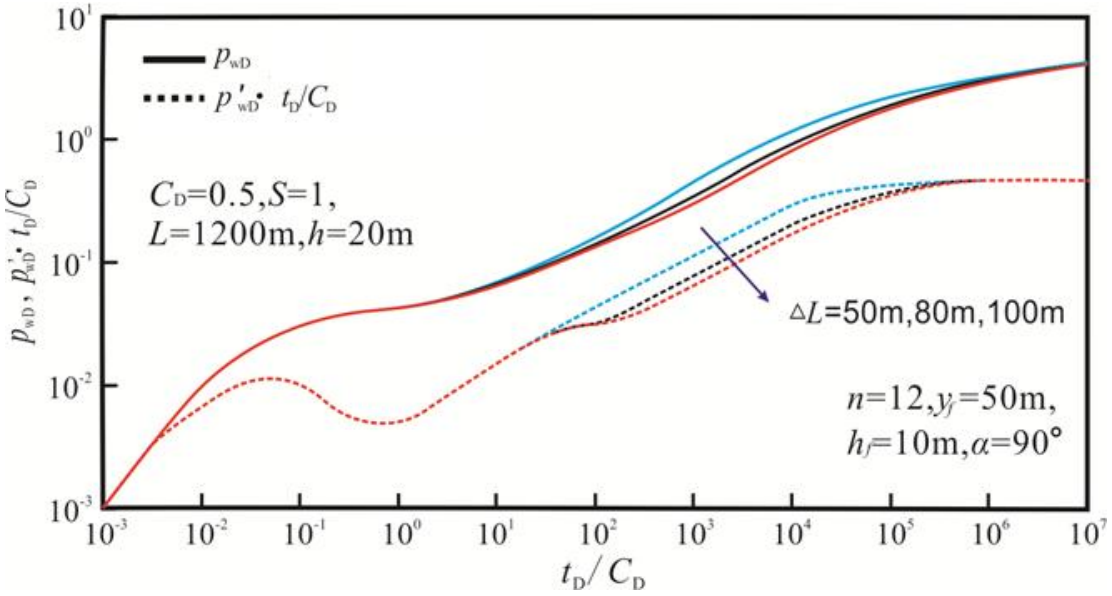

Figure 16, Effect of fracture spacing on multistage fracturing horizontal well test Type curves, which was changed from 50m to 100m.

3.2 Model of finite conductivity fractures

3.2.1 Physical model

We assume a multi-stage fractured horizontal well with (n) finite conductivity fractures lying in a homogeneous reservoir. The physical model is depicted as follows (Lee Shengtai, 1986);

(1) Flow only exists in fractures into the wellbore, flow from the reservoir to the wellbore sections is negligible

(2)The flow from fractures to the wellbore is instantaneous. Flow along the fracture produces pressure drop

(3) Other assumptions are the same with chapter 2.1.1 (Zheng, 1998)

3.2.2 Mathematical model and solutions

During the building process of mathematical model, we assume the unsteady state flow mathematical model of finite conductivity vertical fractures, which is composed of two parts: formation flow and fracture flow. Fractures are assumed as a sink area during formation flow, while the internal flow in the fractures is assumed as one-dimensional flow.

（1）Fracture flow model

The rigorous description of control equations of fracture flow can be written as

$$\frac{\partial^2 P_{\mathrm{f}}}{\partial x^2}+\frac{\partial^2 P_{\mathrm{f}}}{\partial y^2}=\frac{\phi_{\mathrm{f}}\mu_{\mathrm{f}}C_{\mathrm{tf}}}{3.6k_{\mathrm{f}}}\frac{\partial P_{\mathrm{f}}}{\partial t},\quad 0\le x\le x_{\mathrm{f}},0\le y\le\frac{w_{\mathrm{f}}}{2}$$

Initial condition：

$$P_{\mathrm{f}}(r,0)=P_{\mathrm{i}}$$

Fracture symmetry condition：

$$\frac{\partial P_{\mathrm{f}}}{\partial y}(x,0,t)=0$$

Fracture end closure condition：

$$\frac{\partial P_{\mathrm{f}}}{\partial x}(x_{\mathrm{f}},0,t)=0$$

The flow equal condition of the fracture and formation at the fracture surface:

$$\frac{k_{\mathrm{f}}}{\mu}\frac{\partial P_{\mathrm{f}}}{\partial y}(x,\frac{w_{\mathrm{f}}}{2},t)=\frac{k}{\mu}\frac{\partial P}{\partial y}(x,\frac{w_{\mathrm{f}}}{2},t)$$

Down hole flow conditions：

$$4\cdot\frac{k_{\mathrm{f}}h}{\mu}\int_0^{\frac{w_{\mathrm{f}}}{2}}\frac{\partial P_{\mathrm{f}}}{\partial x}(0,y,t)\mathrm{d}y=qB$$

Considering the fracture volume is small, the pressure conductivity coefficient in the fracture is usually $10^{6\sim7}$ times bigger than the value in the formation. Neglecting fracture elastic effect, the fracture flow control equation can be simplified as a steady-state form. Using the flow equal equation of the fracture and formation at the fracture surface, get the integration average of fracture control equation, then the control equation of fracture flow is obtained.

Reuse in the fracture surface, fracture and formation flow under the conditions of the same type of fracture control equation, integral average, get the control equations of fluid seepage problem in the fracture:

$$\frac{\partial^2 P_{\mathrm{f}}}{\partial x^2}+\frac{2k}{k_{\mathrm{f}}w_{\mathrm{f}}}\frac{\partial P}{\partial y}\bigg|_{y=\frac{w_{\mathrm{f}}}{2}}=0,\quad 0\le x\le x_{\mathrm{f}},0\le y\le\frac{w_{\mathrm{f}}}{2}$$

The above equations constitute all the equations of the fracture flow. We introduce several dimensionless variables such as the followings:

Dimensionless fracture pressure: $P_{\mathrm{fD}}=\dfrac{kh}{1.842\times10^{-3}q\mu B}\left(P_{\mathrm{i}}-P_{\mathrm{f}}\right)$ ；

Dimensionless bottom hole pressure: $P_{\mathrm{wD}}=\dfrac{kh}{1.842\times10^{-3}q\mu B}\left(P_{\mathrm{i}}-P_{\mathrm{w}}\right)$ ；

Dimensionless fracture width: $w_{\mathrm{D}}=\dfrac{w_{\mathrm{f}}}{x_{\mathrm{f}}}$；（40）

Dimensionless fracture height: $h_{\mathrm{fD}}=\dfrac{h_{\mathrm{f}}}{h}$；

Dimensionless fracture conductivity: $C_{\mathrm{fD}}=\dfrac{k_{\mathrm{f}}w_{\mathrm{f}}}{kx_{\mathrm{f}}}$。

Using the dimensionless form of the fracture flow equations, we can get:

$$\frac{\partial^2 P_{\mathrm{fD}}}{\partial {x_{\mathrm{D}}}^2}+\frac{2}{C_{\mathrm{fD}}h_{\mathrm{fD}}}\frac{\partial P_{\mathrm{D}}}{\partial y_{\mathrm{D}}}\bigg|_{y_{\mathrm{D}}=\frac{w_{\mathrm{D}}}{2}}=0,\quad 0\le x_{\mathrm{D}}\le 1, 0\le y_{\mathrm{D}}\le \frac{w_{\mathrm{D}}}{2}$$

Initial condition：

$$P_{\mathrm{fD}}\,|_{t_{\mathrm{D}}=0}=0$$

Inner boundary condition：

$$\frac{\partial P_{\mathrm{fD}}}{\partial x_{\mathrm{D}}}\bigg|_{x_{\mathrm{D}}=0}=-\frac{\pi}{C_{\mathrm{fD}}h_{\mathrm{fD}}}$$

Fracture end closure condition：

$$\frac{\partial P_{\mathrm{fD}}}{\partial x_{\mathrm{D}}}\bigg|_{x_{\mathrm{D}}=1}=0$$

The relationship equation of the linear flow and the perpendicular flow from the formation to the fracture surface:

$$q_{\mathrm{fD}}(x_{\mathrm{D}},z)=-\frac{2}{\pi}\frac{\partial P_{\mathrm{D}}}{\partial y_{\mathrm{D}}}\bigg|_{y_{\mathrm{D}}=\frac{w_{\mathrm{D}}}{2}}$$

Double integral the flow control equation we can get:

$$p_{\mathrm{wD}}-p_{\mathrm{fD}}(x_{\mathrm{D}})=\frac{\pi}{C_{\mathrm{fD}}h_{\mathrm{fD}}}(x_{\mathrm{D}}-\int_0^{x_{\mathrm{D}}}\int_0^{v}q_{\mathrm{fD}}(u)dudv)$$

（2）Coupling model of reservoir and fracture

The reservoir pressure and fracture pressure are equal at j fracture surface. Inlet the bottom hole pressure p_D of infinite conductivity multi-fractured horizontal wells we obtained in section 2.1:

$$P_{\mathrm{fD}}(x_{\mathrm{D}})=P_{\mathrm{D}}(x_{\mathrm{D}},0,z)+S_{\mathrm{f}}q_{\mathrm{fD}}(x_{\mathrm{D}},z)$$

Inlet (47) into the fracture pressure equation:

$$p_{\mathrm{wD}}-[P_{\mathrm{D}}(x_{\mathrm{D}},0,z)+S_{\mathrm{f}}q_{\mathrm{fD}}(x_{\mathrm{D}},z)]=\frac{\pi}{C_{\mathrm{fD}}h_{\mathrm{fD}}}(x_{\mathrm{D}}-\int_0^{x_{\mathrm{D}}}\int_0^{v}q_{\mathrm{fD}}(u)dudv)$$

In addition, for constant production wells, the fracture flow integral normalized relations are:

$$\sum_{j=1}^{m}\int_{-x_D}^{x_D}q_{\mathrm{jfD}}(u)du=1$$

In addition, the final pressure equation obtained is the Fredholm integral equation, which is difficult to get the analytic solution and can only be solved

discretely by numerical method.

As shown in Figure 17, we divided the half wing of fracture j into N sections equally, with a length of x_f / N for each section. So, the 1st section is from 0 to x_f / N, the 2nd, from x_f / N to $2x_f / N$; the i section is from $(i-1)x_f / N$ to ix_f / N, the last section, from $(N-1)x_f / N$ to x_f. And we assume the rate at fracture i is q_{ji}(i=1，2，…，N).

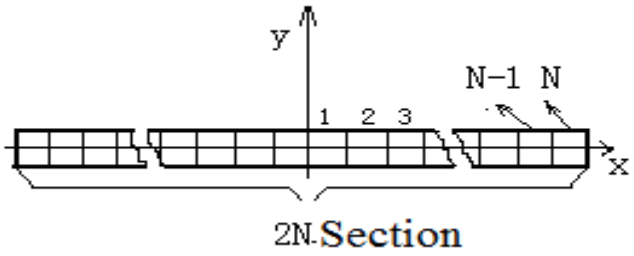

Figure 17 Sketch map of the fracture piecewise discretation

After equation discretization, we can get a linear equation group of m×N+1 order about p_{wD} and q_{jDi}，i=1,2,...N, from which we can get the bottom hole pressure $\overline{P}_{wD}$ after considering the wellbore storage of a multi-stage horizontal well with finite conductivity fractures in a homogeneous reservoir.

Finally we inlet $\overline{P}_{wD}$ into Duhamel superposition formula and get the bottomhole pressure equation considering the wellbore storage of a multi-stage horizontal well with finite conductivity fractures in a homogeneous reservoir.

3.2.3 Type curves

In the infinite conductivity model, we have discussed the influence of the skin factor, wellbore storage coefficient, fracture numbers, fracture half length, fracture space and other factors. In the following we will specially discuss the effects of dimensionless fracture conductivity.

Figure 18 is the theoretical pressure and derivative type curves as fracture

conductivity varies from 5; 10; 50 to 100. As can be seen from the Figure, in case of other parameters are not changed, the smaller the dimensionless fracture conductivity is, the more obvious the bilinear flow period shows. This is mainly caused by the linear flow from formation to fractures that are more obvious than inside fractures as the dimensionless fracture conductivity is getting smaller.

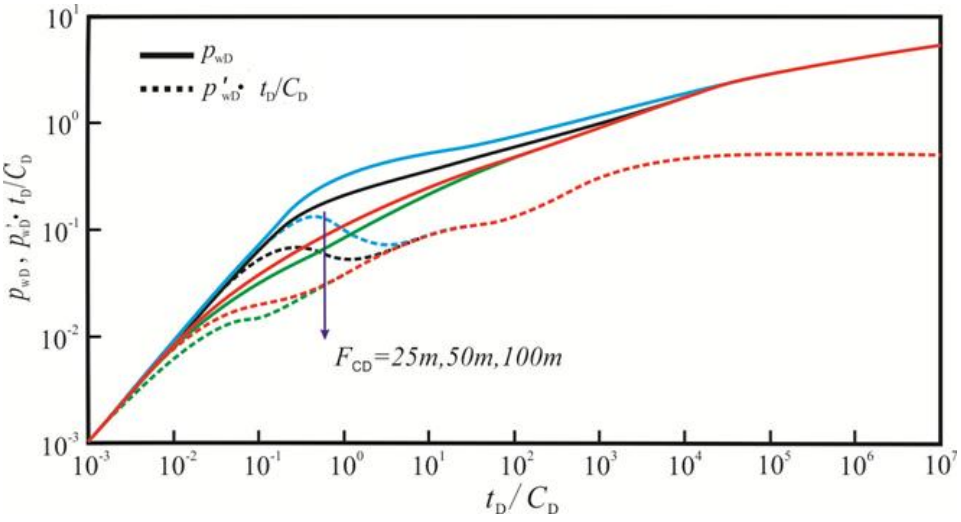

Figure18, Influence of fracture conductivity, dimensionless F_{CD} to the multi-fracture type curves, which was changed from 25m; 50m and 100m.

3.3 The general principle of type curve match

In well test analysis, there is a quantitative proportional relationship between dimensionless and dimension parameters. And the coefficient of proportionality only refers to several reservoir and logging parameters. Such as:

Dimensionless pressure：

$$P_D = \frac{kh}{0.001842qB\mu}\left(P_i - P_{wf}\right)$$

Dimensionless time：

$$t_D = \frac{3.6k}{\phi\mu C_t r_w^2}t$$

Dimensionless wellbore storage：

$$C_D = \frac{C}{2\pi\phi C_t r_w^2 h}$$

$$\frac{t_D}{C_D} = 22.61947 \frac{kh}{\mu} \cdot \frac{t}{C}$$

Where: C—Wellbore storage，m^3/MPa；

q—oil rate，m^3/d。

The meaning and unit of other parameters are the same as those defined in the previous section.

By the definition of dimensionless parameters above, the dimensional equations and the boundary conditions of well test analysis can be turned into dimensionless equations, which will have no relation with reservoir characteristics. In other words, it is a generic model.

Dimensionless parameters on a log scale:

$$\log P_D = \log \Delta P + \log \frac{kh}{0.001842 qB\mu}$$

$$\log \frac{t_D}{C_D} = \log t + \log\left(22.6194 \frac{kh}{\mu} \cdot \frac{1}{C} \right)$$

where： $\Delta P = P_i - P_{wf}$

As we can see from the two equations above, the practical and theoretical curve shape is exactly the same when using the correct model. As can be seen from the equation above, the two curves should match completely through coordinate transformation, which reflects some important characteristic parameters of the formation and well and therefore we can get all reservoir parameters in this way. Since

$$\log \frac{P_D}{\Delta P} = \log \frac{kh}{0.001842 qB\mu}$$

$$\log \frac{t_D}{t} = \log \frac{3.6k}{\phi\mu C_t r_w^2}$$

Then, we can get the match value： $\Delta P = (P_D / \Delta P)_M, (t_D / t)_M$ ： So the permeability is:

$$k = \frac{0.001842 qB\mu}{h}\left(\frac{P_D}{\Delta P}\right)_M$$

If the type curves also considering other parameters, such as S, C etc., their values can be calculated in the same way.

Calculation of reservoir parameters：

① By pressure match， we can get k：

$$k = \frac{0.001842 qB\mu}{h}\left(\frac{P_D}{\Delta P}\right)_M$$

② By time match， we can get wellbore storage C：

$$C = 22.61947\frac{kh}{\mu}\cdot\frac{1}{\left(t_D / C_D / \Delta t\right)_M}$$

③ By type curve match, we can get Skin：

First：

$$C_D = \frac{0.1592}{\phi C_t h r_w^2} C$$

$$S = 0.5\ln\frac{\left(C_D e^{2S}\right)_M}{C_D}$$

By type curve matching, we can get radial flow straight line between starting and end point. In the dimensionless derivative curve, when the measured derivative points just turns to P_D equals 0.5, the radial flow starting point begins. When it leaves the 0.5 line, the radial flow ends.

Through type curve match interpretation and parameter adjustment, we can complete well test interpretation work. As the summary, the match interpretation procedures are shown in Figure 19 below:

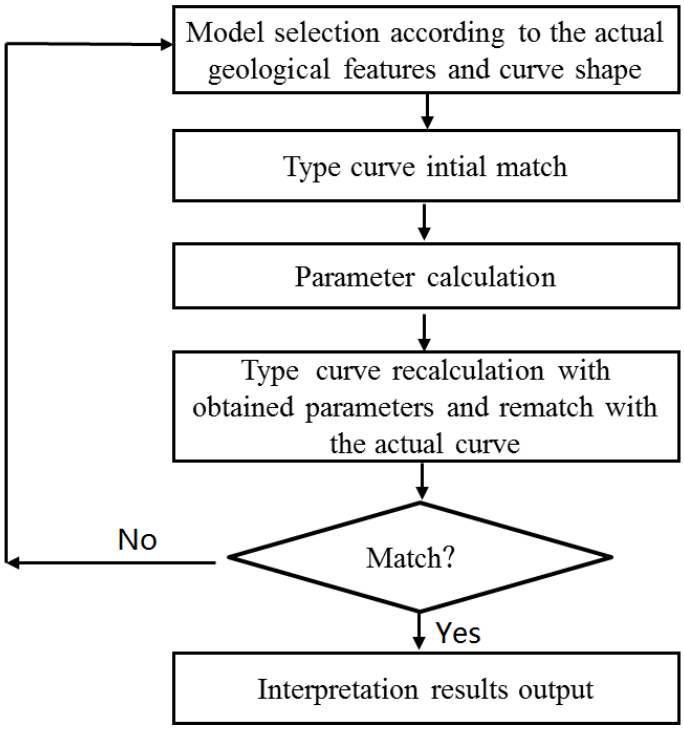

Figure19, Multi fractured horizontal well test interpretation procedures/flowchart.

Chapter 4

Field application

Field example：Well 1 well testing and data interpretation

(1) The well profile and basic data

Well 1 is a long well section horizontal well with successfully multistage subsection fracturing in low permeability reservoir. With the production close to 3000m^3. The barefoot interval is 2850-4014m， Horizontal section length is 1221m，which was fractured in 12 sections.

Production with 9mm flow choke, the tubing pressure is 3.8MPa， with water content of 57.5%, the daily fluid production rate is 183.6m^3.

Table 1 listed the basic data of Well 1, Figure 20 shows the fracturing pipe string structure/completion, Figure 21-22 is the well 1 plan view showing horizontal well path with fracture sections, and Micro fracture seismic image monitoring results of Well 1, the microscopic fracture image monitoring results include the fracture azimuth、the main fracture length and the main fracture height of total 12 sections, which are listed in table 2.

Table 1Basic data table of Well 1

well pattern：production well	well type：horizontal well
Technology casing size and depth： 177.8mm×2842.86m	structural location：/
Max hole deviation and depth： 92.60°×3399.83m	hole deviation location：337.10°
well completion method：open hole	slant depth of finishing drilling：4066.00m
horizon：Es3	well section：2850.000～4014.00m
thickness：15m	porosity：14.9%
permeability：$1.1\times10^{-3}\ \mu m^2$	

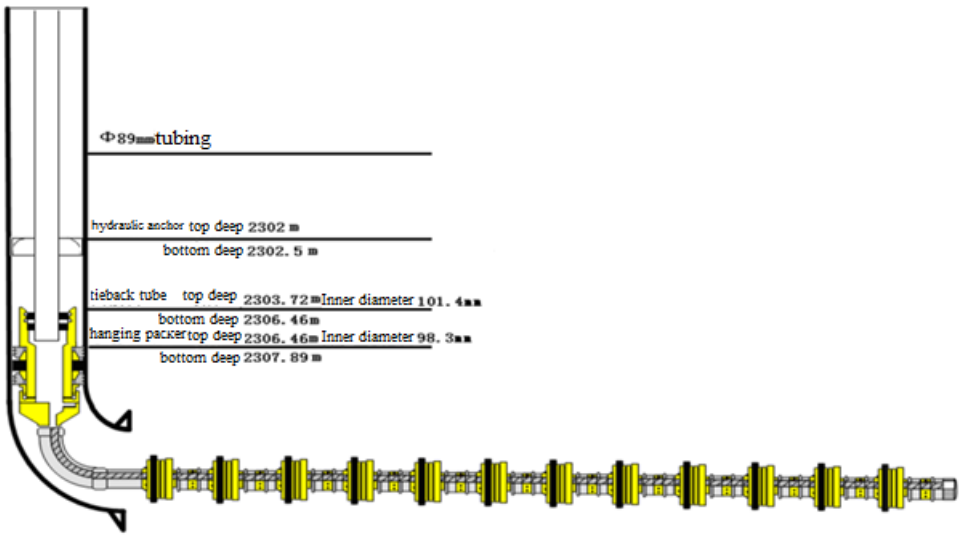

Figure 20, Fracturing pipe string construction/completion of Well 1, where packers separated sections, which are due to be fractured (12 sections in total).

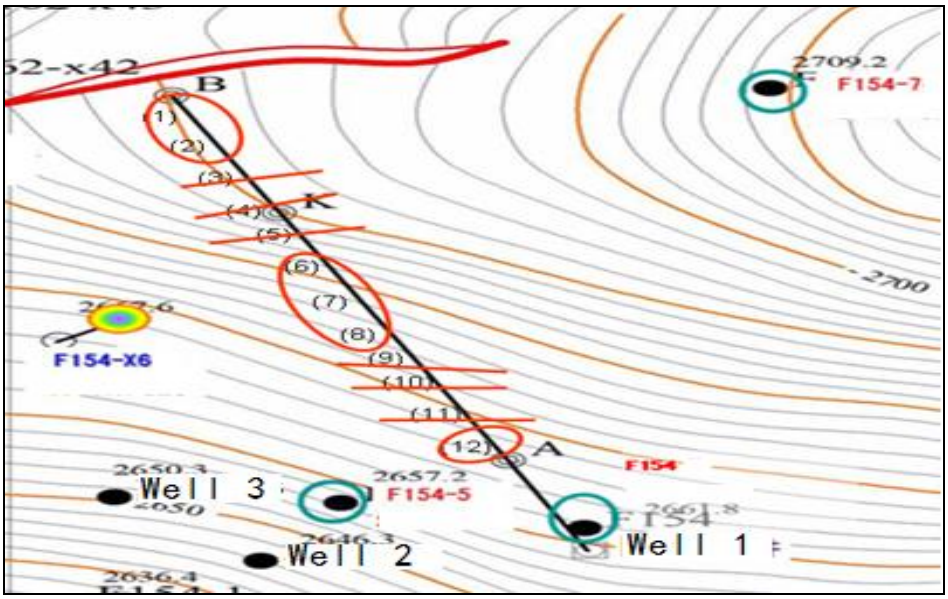

Figure 21, The well 1 plan view showing horizontal well path with fractures sections, where the solid black line denotes the horizontal well path, along with the fractured sections denoted in solid red lines and circles (1-12). The well testing model developed was applied to interpret the testing pressure data from this well, and proved to be applicable.

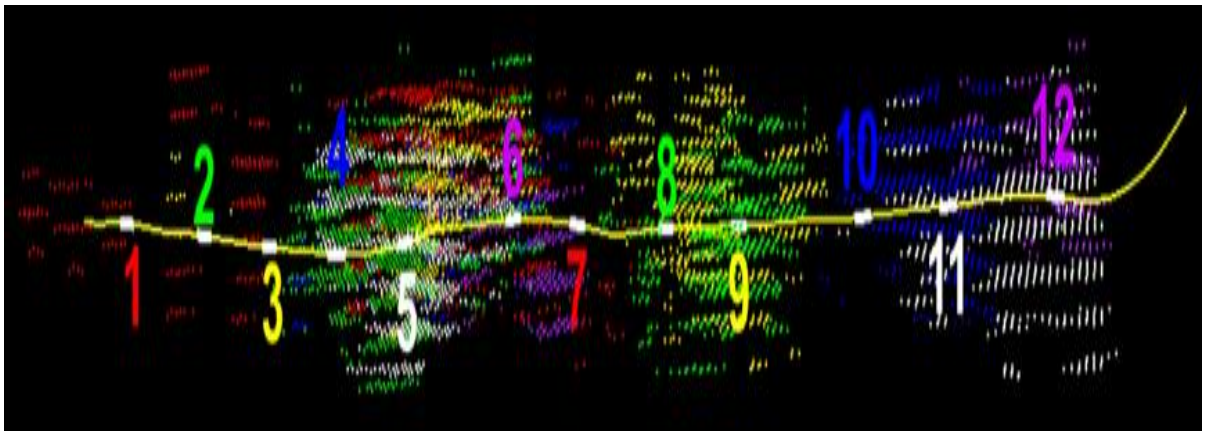

Figure 22, Micro crack seismic image monitoring results - well test Type curves of Well 1, where effectively fractured sections and less fractured sections are clearly shown, as consistently marked in the previous Figure 21. Clearly the developed math model treated both horizontal well path and fractures, on average, "ideal", but the analysis on testing data produced good matching results as shown in Figs 23 - 24 respectively.

Table 2 Micro crack image monitoring results of Well 1

During fracturing	fracture azimuth	The main crack length(m)	The main crack height(m)	shape	remark
1	NE120°	300	20	multi-blade	Including pressure test

2	NE65°	450	25	Multiple branch Wing	
3	NE40°	250	25	two flanks	
4	NE70°	230	20	multi-blade	
5	NE150°	350	40	single-blade	
6	NE90°	270	40	multi-blade	
7	NE125°	350	35	Multiple branch Wing	
8	NE20°	300	35	multi-blade	
9	NE35°	480	35	two flanks	
10	NE85°	200	35	Multiple branch Wing	
11	NE100°	230	30	Multiple branch Wing	
12	NE50°	200	30	two flanks	

(2) Well test interpretation results

Based on the basic reservoir data and pressure testing data of Well 1，using the model of homogeneous infinite-conductivity multi fractured horizontal well with closed top and bottom boundaries，the analysis results from the interpretation are shown in Figure 23-24，the well test interpretation results are listed in table 3，derived parameters of fractures are listed in table 4.

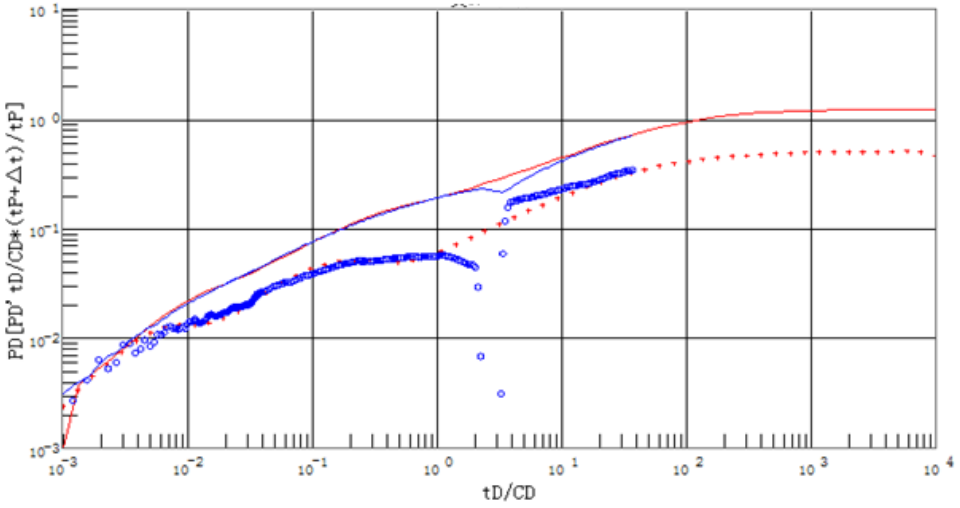

Figure 23, Matching/fitting a double logarithmic graph of Well 1. The blue solid and circle lines denote both pressure and associated logarithmic derivatives of the field test data, while the red solid and dotted lines denote both pressure and logarithmic derivatives from the developed math model analytical solution. The matching of the two sets is fairly good enough to justify the derived results as listed in Table 3. The "sharp" drop on both pressure and the associated derivatives are more likely the mechanic "noise" from test operation, rather than reservoir behavior. This phenomenon is rather common with the field data.

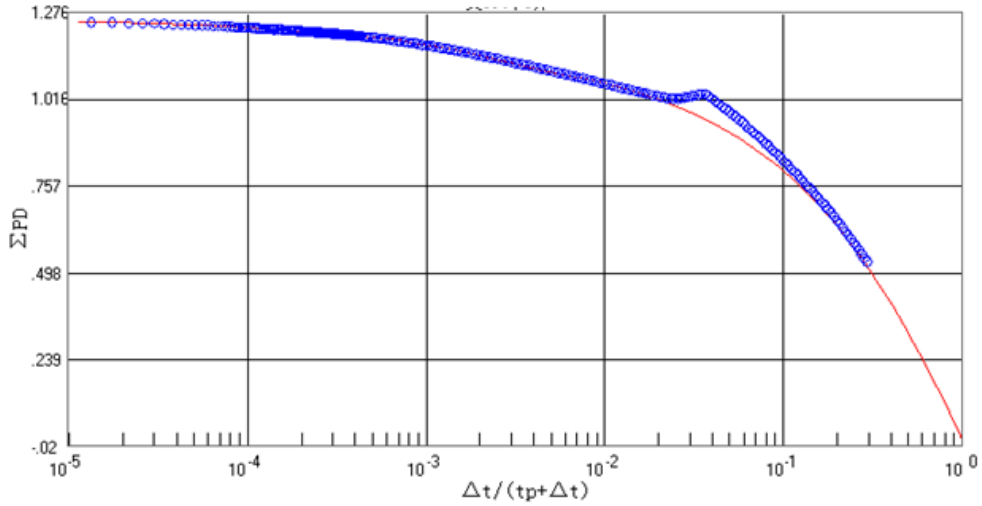

Figure 24, Matching/fitting a semi logarithmic graph of Well 1. This is standard Horner time plot showing a match between filed data (blue) and analytical solution (red). The mechanic "noise" observed from the previous Figure 23 is still visible here at the 4th log cycle of time between 10^{-2} - 10^{-1}.

Table 3 Well test interpretation results table of Well 1

reservoir model	infinite-conductivity multi fractured	the ratio of horizontal permeability to verticalk_h/k_v	10
Well model	well bore storage—skin	vertical permeabilityk_v ($\times10^{-3}\mu m^2$)	0.165
Outer Boundary model	infinite	formation pressureP_i(MPa)	32.15
internal boundary model	error function changing well bore storage	effective length of horizontal well(m)	1224
permeability ($\times10^{-3}\mu m^2$)	1.65	Flow pressure P_w(MPa)	26.71

formation factor(/kh)	0.026	pressure difference (MPa)	5.44
flow coefficient(/μ)	0.0371	flow efficiency	1.992
Skin factor	1.166	pressure conductivity coefficient (μm^2.MPa/mPa.s)	16.64
well bore storage factor (m^3/MPa)	3.855		

Table 4 parameters of fractures results table of Well 1

No. of fracture *n*	crack spacing*D*(m)	fracture dip*α*(°)	Half length x_f(m)	Upper part height h_{fs}(m)	Lower part height h_{fx}(m)
1	300	60	85	7.5	7.5
2	200	65	70	7.5	7.5
3	200	50	65	7.5	7.5
4	200	70	70	7.5	7.5
5	200	60	80	7.5	7.5
6	100	90	100	7.5	7.5

This well was fractured to 12 sections，by model discrimination，we found that，the best fitting result is the case when the number of fractures is six. With this in mind，considering the communication between micro fractures， the 12 fractures series were connected to each other，that has formed 6 main fracture zone，each of which shows a fracture characteristics on the double logarithmic pressure derivative curve. The micro seismic monitoring results graph also shows that the hydraulic fracturing formed several high density fractured zones（Figure 21-22）.

Chapter 5

Conclusions and Future work

(1) Considering the condition that fracture flow pattern with uniform flow, finite-conductivity and infinite-conductivity，the condition that fracture fully penetrated or partly penetrated，the condition that perforation on fractures or between fractures，considered the fracture dip and different attributes of each fracture etc.，We build the well test interpretation model for multi-fractured horizontal well. The model considers more variable factors which can be used in a more comprehensive applicable range of field conditions. So it has an obvious advantage when interpreting the fractured horizontal well test data.

(2) Multi stage fractured horizontal well type curves reflect 5 main flow regimes, where the fracture linear flow and fracture pseudo-radial flow are mainly controlled by several parameters such as the fracture height, fracture half length and fracture dip angle. Besides, the parameters such as arbitrary angle fracture, fracture spacing, partially perforated reservoir, asymmetrical fracture half length, etc. also have obvious influence on the well test response and should not be ignored. The longer the fracture half length is, or the shorter the fracture spacing, the earlier the interference between fractures shows, and the shorter the fracture pseudo radial flow section lasts, or even disappear.

(3) With the established well test interpretation model of multi-stage fractured horizontal well, we have taken a field data sets for application and obtained the characteristic parameters of the reservoir and fractures. Field application shows that, developed well testing model can meet the actual production requirement. The interpretation result meets the demand of the evaluation of the unconventional tight oil and gas reservoirs.

(4) The current developed model and solutions are limited to the ideal assumptions, more realistic approaches should be made further, when more field data are available in the future.

Nomenclature

a_1, a_2, b_1, b_2 = distance from the well to the Boundary, m

C = well bore storage factor, m^3/MPa

C_D=dimensionless well bore storage factor

C_{FD} = dimension less perveance

C_t =composite compressibility, MPa^{-1}

$E(\ )$=characteristic function

$F(\ )$=orthogonal transformation

h = reservoir thickness, m

h_{fd} = Lower part height of fracture, m

h_{fu}= Upper part height of fracture, m

h_w= height from the horizontal well to the bottom surface, m

h_{fdD} = dimensionless Lower part height of fracture

h_{fuD} = dimensionless Upper part height of fracture

J = productivity index,m^3/(MPa.d)

k_x, k_y, k_z = permeability of x, y, z direction, μm^2

L= horizontal well length, m

L_D= dimensionless horizontal well length

p = pressure, MPa

p_i = initial formation pressure, MPa

p_w= bottom hole pressure, MPa

p_D= dimensionless pressure

p_{wD}= dimensionless bottom hole pressure

q = point source production, m^3/d

q = total production, m^3/d

q_j= production of the fracture j, m^3/d

q_D= dimensionless production,

q_{Dj}= dimensionless production of the fracture j,

r_w= well radius, m

s= Laplace variables

S = skin factor

S_f = skin factor of the fracture

t= time, h

t_D= dimensionless time

y_f=half length of the fracture, m

ΔL_i =distance from the fracture j-1 to the fracture j, m

ΔL_{Di} = dimensionless distance from the fracture j-1 to the fracture j

x, y, z = three dimensional coordinate, m

x_w, y_w, z_w= three dimensional point source coordinate

x_{mj}, y_{mj}, z_{mj}= intersection point coordinate of the horizontal well and fracture j

x_{0j}, y_{0j}, z_{0j}= endpoint coordinate of the fracture j

α= fracture dip, °

α_j= fracture dip of the fracture j, °

$\delta(\ )$=δ function

μ = viscosity, mPa·s

$\emptyset$ = porosity

λ_β, λ_γ, λ_n = characteristic value of the direction x, y, z

$\lambda_{\beta\gamma n}$ = three dimensional characteristic va

References

[1] Guo, G. and Evans, R.D. Pressure-transient Behavior and Inflow Performance of Horizontal Wells Intersecting Discrete Fractures[C]. SPE26446, 1993.

[2] Al Rbeawi, S. and Tiab, D. Transient Pressure Analysis of a Horizontal Well With Multiple Inclined Hydraulic Fractures Using Type-Curve Matching[C].SPE149902, 2012.

[3] Chen Wei, DuanYonggang, HuangCheng, XieJu. Well Test Analysis of Hydraulic Fractured Well with a Horizontal Fracture [J]. WELL TESTING. 2000, 9(3):8-11.

[4] Li Yongming, ZhaiRui, GaoRuimin et al. Study of pressure decline on horizontal well after multiple-stage fracturing [J]. Petroleum Geology and Recovery Efficiency, 2012, v.19; 97(4): 66-70.

[5] FAN Dong-yan, YAO Jun, WANG Zi-sheng et al. Well testing on fractured horizontal well with different dip angles [J]. Journal of Hydrodynamics(Ser.A), 2009,v.24(6):705-712.

[6] Sheng Ruyan, Liu Hua, Xiang Xiyong et al. Performance analysis of fractured horizontal wells in tight gas reservoir [J]. Petroleum Geology and Recovery Efficiency, 2003(1):40-42.

[7] Zerzar, A. and Bettam, Y. Interpretation of multiple hydraulically fractured horizontal wells in closed systems [C]. SPE 84888, 2003.

[8] Brown, M., Ozkan, E., Raghavan, R. et al. Practical solutions for pressure transient responses of fractured horizontal wells in unconventional reservoirs[C]. SPE 125043, 2009

[9] Zhang Ziming, Current Development Situation of Fracturing Technology in Horizontal Wells [J]. Sino-Global Energy, 2009(9):39-44.

[10] Roumboutsos, A., Stewart, G.., A direct deconvolution or convolution algorithm for well test analysis [C]. SPE 18157, 1988.

[11] Stehfest, H.: Numerical inversion of Laplace transform - algorithm 368, Communication of the ACM, 13(1), 47-49, 1970.

[12] Economides. Observations and Recommendations in the Evaluation of Tests of Hydraulically Fractured Wells [R]. SPE16396, 1987: 49- 60.

[13] Lee Shengtai, Brockenbrough J R., A New Approximate Analytic Solution for Finite-Conductivity Vertical Fractures [J]. SPE Formation Evaluation, 1986, 1(1):75- 88.

[14] Zheng Shiyi, Lili Xue, An Advanced Multi-lateral Horizontal Well Coupled Coalbed Methane (CBM) Simulation Model and its Application in Qinshui Basin of China[C] SPE-149956-MS

[15] Zheng Shiyi, Patrick Corbett, George Stewart, the Impact of Variable Formation Thickness on Pressure Transient Behavior and Well Test Permeability in Fluvial Meander Loop Reservoirs[C] SPE-36552-MS, 1996

[16] Zheng Shiyi, Diagnosis and Analysis of Nonlinear Transient Pressure From Permanent Down hole Gauges (PDG)[C] SPE-134761-MS,2011

[17] Zheng Shiyi, Xiaogang Li, Transient pressure analysis of 4D reservoir system response from permanent down hole gauges (PDG) for reservoir monitoring, testing and management[C] SPE-109112-MS,2007

[18] Zheng Shiyi, Fei Wang, Extraction of Interference from Long Term Transient Pressure Using Multi-Well Deconvolution Algorithm for Well Test Analysis[C] SPE-131294-MS, 2010